remote sensing

MDPI

Article

The Importance of High Resolution Digital Elevation Models for Improved Hydrological Simulations of a Mediterranean Forested Catchment

João Rocha [1,*], André Duarte [1], Margarida Silva [1], Sérgio Fabres [1], José Vasques [2], Beatriz Revilla-Romero [3] and Ana Quintela [1]

1 RAIZ—Forest and Paper Research Institute, Quinta de S. Francisco, Rua José Estevão (EN 230-1), Eixo, 3800-783 Aveiro, Portugal; andre.duarte@thenavigatorcompany.com (A.D.); margarida.silva@thenavigatorcompany.com (M.S.); sergio.fabres@thenavigatorcompany.com (S.F.); ana.quintela@thenavigatorcompany.com (A.Q.)

2 Navigator Forest Portugal, Zona Industrial da Mitrena, 2910-738 Setúbal, Portugal; jose.vasques@thenavigatorcompany.com

3 Remote Sensing and Geospatial Analytics Division, GMV, Isaac Newton 11, P.T.M. Tres Cantos, E-28760 Madrid, Spain; brevilla@gmv.com

* Correspondence: joao.rocha@thenavigatorcompany.com

Received: 27 August 2020; Accepted: 8 October 2020; Published: 10 October 2020

check for updates

Abstract: Eco-hydrological models can be used to support effective land management and planning of forest resources. These models require a Digital Elevation Model (DEM), in order to accurately represent the morphological surface and to simulate catchment responses. This is particularly relevant on low altimetry catchments, where a high resolution DEM can result in a more accurate representation of terrain morphology (e.g., slope, flow direction), and therefore a better prediction of hydrological responses. This work intended to use Soil and Water Assessment Tool (SWAT) to assess the influence of DEM resolutions (1 m, 10 m and 30 m) on the accuracy of catchment representations and hydrological responses on a low relief forest catchment with a dry and hot summer Mediterranean climate. The catchment responses were simulated using independent SWAT models built up using three DEMs. These resolutions resulted in marked differences regarding the total number of channels, their length as well as the hierarchy. Model performance was increasingly improved using fine resolutions DEM, revealing a bR^2 (0.87, 0.85 and 0.85), NSE (0.84, 0.67 and 0.60) and Pbias (−14.1, −27.0 and −38.7), respectively, for 1 m, 10 m and 30 m resolutions. This translates into a better timing of the flow, improved volume simulation and significantly less underestimation of the flow.

Keywords: forested catchment; forestry; hydrological modeling; SWAT model; DEM

1. Introduction

Forests play a significant role on the hydrological cycle and have a key importance on ecosystems regulation. Planted forest productivity is highly dependent on water availability [1]. Therefore, the evaluation of watersheds' hydrological response is important especially in regions that, under present day conditions, register water restrictions such as the Mediterranean bioclimatic zones [2,3]. In Portugal, forests cover about 36% of the total mainland area [4], holding an important role on the environment and on the national economy.

In order to obtain insight on hydrological responses and on water availability at a catchment scale, hydrological models may be used. These models require, as an input, a morphological surface representation, and the digital elevation model (DEM) is one of the most common. DEM is a numeric representation of a surface arranged in a set of regular grids each containing the three-dimensional

(3D) (x, y, z) coordinate records [5]. A DEM may be produced based on three arrangements: contour lines (x, y data on equal elevation lines); triangular irregular network (non-overlapped linked triplets of nodes with x, y, z data); or mass points (x, y, z data regularly or irregularly distributed) [6].

DEM data sources are typically obtained by using: (i) remote sensing techniques on which the sources may be Interferometric Synthetic Aperture Radar (IfSAR), either from the Shuttle Radar Topography Mission (SRTM), Advanced Spaceborne Thermal Emission or Reflection Radiometer; (ii) photogrammetry with stereo pairs of aerial imagery (e.g., satellite, airborne and Unmanned Aerial Vehicles); (iii) laser scanning by Light Detection and Ranging (LiDAR); (iv) interpolated global positioning system and total stations; and (v) cartographic digitalization on pre-existing topographic (contour) maps [7,8]. Photogrammetry, IfSAR and LiDAR are preferential sources to produce DEMs [9,10].

From the DEM it can be extracted geomorphological and hydrological data (e.g., aspect, slope, stream network, watershed delineation, flow direction and accumulation patch) and, therefore, the horizontal and vertical resolutions of the DEM will impact on the accuracy of the linked extract products. As concluded by Sørensen et al. [11] and Vaze et al. [12], the input DEM (accuracy and resolution) will impact the ranges of hydrological and topographic indices derived from the DEM. Following Tan et al. [13,14] and Xu et al. [15], DEM uncertainties are linked with the input resolution (provided by the data sources) and the applied resampling techniques.

Physically based semi-distributed and distributed hydrological models are powerful tools to simulate catchment processes and linked responses. Moreover, hydrological models may be used to support effective land management and planning of forest resources. They can be used as effective decision support tools [16,17] to set site-specific forestry management practices.

The Soil and Water Assessment Tool (SWAT) is a continuous time, physical based and semi-distributed ecohydrological model that simulates on a daily basis landscape processes and watershed responses [18,19]. The model has been widely used for three decades and it has been applied to assess different inputs and scenarios for multiple variety of catchments and objectives (e.g., climate change impacts, land use and land cover changes, water quality and quantity, sediment exportation, management practice effects) resulting in more than 3900 published research papers [20]. The SWAT model has been successfully used to address the impacts of different resolution input data on catchments and hydrological responses [21–23] and some studies have focused on the use of low to high resolution input DEM to assess SWAT performance and simulation results [24–27]. The links between different input DEM resolutions and the uncertainty on model predictions have been discussed in other research studies [28–30].

SWAT procedures that are DEM-dependent (e.g., watershed delineation, stream network definition, sub-basins) will be largely constrained by the DEM resolution and uncertainty. Additionally, as stressed by Goulden et al. [31], the lack of knowledge on DEM uncertainty and the potential undefined cascade impact on hydrological model simulations may result in inaccurate assumptions and under or overestimated conclusions for the modeler. Wu et al. [32] applied the SWAT to 10 catchments and used three DEM resolutions (250 m, 500 m and 1000 m) to assess the links between automatic watershed extraction (from DEM), watershed parameters and area threshold values. They concluded that a DEM resolution increase results in a more refined flow direction and accumulation calculation, meaning a more realistic representation of the stream network.

Tan et al. [13] found that SWAT generated stream network was set to be more sensitive with regard to the DEM resolution rather than DEM source or the applied resampling technique. Furthermore, Tan et al. [14] obtained better streamflow simulations using 20 m and 60 m resolution DEMs as well as improved DEM sensitivity analysis upon the integration of the smallest area threshold (1000 ha) value.

Camargos et al. [33] debated the use of fine (regional data) and coarse (global data) detail inputs to improve the robustness of SWAT model simulations. Zhang et al. [29] and Xu et al. [15] analyzed the influence of contrasting DEM resolutions on SWAT simulations for hydrological responses and nutrient exports. Goulden et al. [24] presented a comprehensive analysis on DEM resolution and sensitivity of the SWAT outputs, namely the increase of slope class with higher DEM resolutions and the linked increase of sediments loads as a consequence of the reduction on watershed areas using higher resolutions.

The great majority of SWAT modeling studies explicitly fails to consider the simulations on forest dominated catchments despite the relevance of these ecosystems and provided services. In addition, there is also a gap on studies that focus on forest dominated catchments on water scarce regions under the influence of Mediterranean-type climate.

This study focuses on the use of DEMs with different resolutions to improve the accuracy of hydrological modeling in a forest dominated catchment in a water scarce region in Alentejo (Portugal). To this end, the SWAT model was applied on relative flat catchment with three DEM cell sizes (1 m, 10 m and 30 m) in order to simulate the impacts of different DEMs on the representation of watershed characteristics, processes and responses.

There are two major research questions that we intend to address: What is the impact of different DEM resolutions on surface representation and watershed properties in a flat area? Is it worthwhile to use very high resolution DEMs to simulate catchment processes and responses in a forest dominated catchment under the influence of Mediterranean climate?

2. Material and Methods

2.1. The Study Area

The Caniceira catchment (is located in Alcolobre river basin (in the context of the wider Tagus transboundary river basin), in the Alentejo region in mainland Portugal. The catchment is under the influence of a Mediterranean climate and registers an average annual precipitation of about 720 mm with a dry warm summer and a mild winter and it is characterized by a temperate with dry and hot summer climate (Csa) according to the Köppen classification [34] (Figure 1). In addition, it is categorized as a sub-humid mesothermal, registering a severe water-deficit, especially during summer time (C2 B′2) [35,36]. The catchment is located in a relatively flatten area with elevations ranging from 99 to 164 m (above sea level) and covers an area of about 267 ha.

Regarding the geological background, the catchment is located in the context of the Lower Tagus Tertiary basin, whose genesis is related to Pyrenean compression [37]. The catchment is dominated by Miocene and Pliocene fluvial sedimentary deposits, conglomerates and reddish to yellowish clay sandstones and some Quaternary sands and gravels beds. The Tertiary deposits overlay in discordance with the gneiss and migmatite formations from Precambrian [38]. The hydrogeological context of the area is associated with an extensive multilayered aquifer system, shaped by variable in depth layers of sandstones alternating with impervious clay layers [39,40].

Following the Portuguese soil classification [41,42] and the FAO-UNESCO classification [43,44], the catchment soils are mainly Arenic Endoleptic Regosols and Arenic Epileptic Regosols, with little or no profile differentiation, on which bedrock is located between 25 cm and 50 cm (Epileptic) or between 50 cm and 100 cm (Endoleptic) with sandy or coarser texture.

This is a forest dominated catchment largely occupied by evergreen broadleaf species (*Eucalyptus globulus*, *Quercus suber*—cork oak, *Quercus faginea*—green oak, *Pinus pinaster*—maritime pine; Table 1) and by sclerophyllous vegetation (Mediterranean scrubland). The catchment is linked to a riparian gallery of high nature conservation value, including alders and narrow-leaved ash as the most common tree cover and otter, polecat and Eurasian sparrowhawk as faunistic representatives. The land use and land cover data (1:10 scale) was obtained with field observation and detailed mapping survey validated with pan-sharped World-View-2 orthoimage from 8 August 2019.

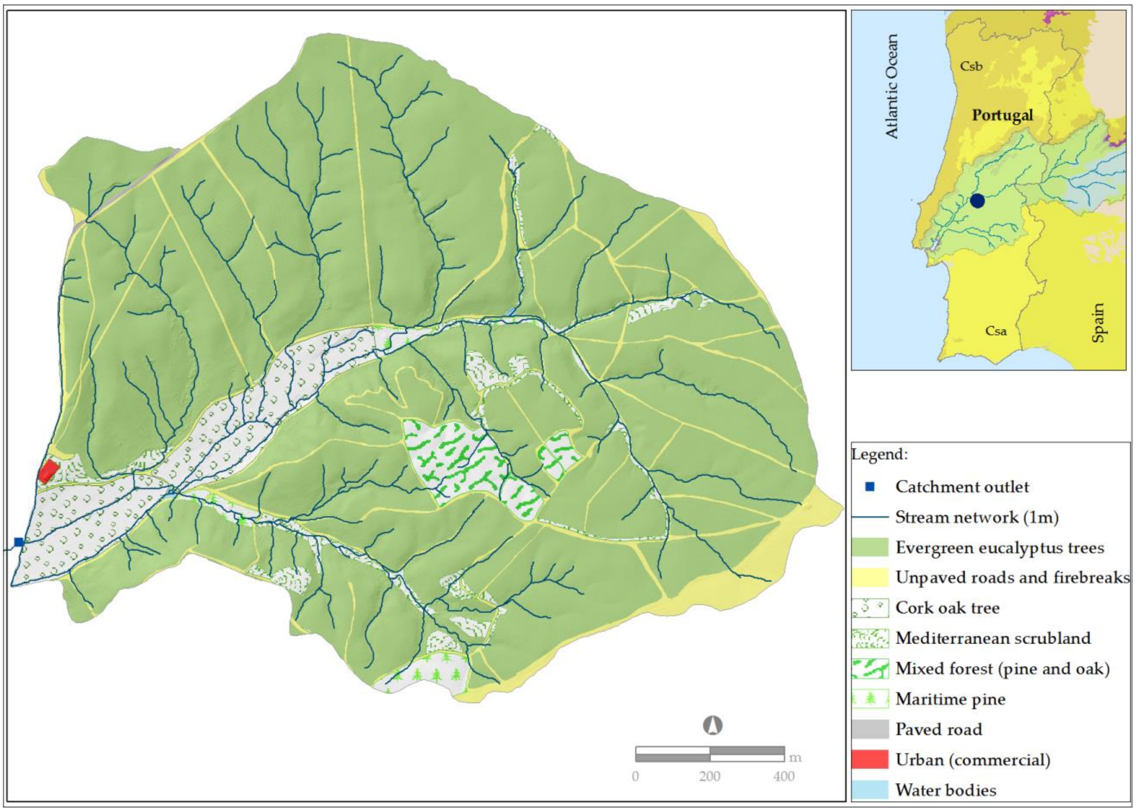

Figure 1. Land cover and stream network (1 m resolution) at Caniceira catchment, in the context of the Tagus transboundary river basin with the Köppen classification (top right map).

Table 1. Land use and land cover (LULC) distribution at Caniceira catchment.

LULC	Area ha	Area %
Eucalyptus	210.9	78.9
Unpaved roads and firebreaks	19.9	7.4
Cork oaks	16.4	6.1
Mediterranean scrubland	9.2	3.4
Mixed forest (maritime pine, green oak)	6.3	2.4
Maritime pine	3.7	1.4
Paved road	0.4	0.2
Urban (commercial)	0.2	0.1
Water bodies	0.1	0.0

2.2. DEM Input Data

The DEMs used as input in the SWAT model were obtained using: Synthetic Aperture Radar interferometric data, GPS and digitalization surveys and Airborne Laser Scanning surveying data.

The SRTM from 2000 in combination with the United States Geological Survey's GTOPO30 data set, provided about 80% worldwide coverage of the SAR interferometric data, which were resampled at 1 arc-second resolution (~30 m × ~30 m) [45]. The SRTM-DEM was validated for Portugal [46,47] and is freely available. In addition, it has been used worldwide as an input DEM in the SWAT model [28,48,49].

The 10 m resolution DEM was based on the contour lines data (National Cartography Series—1:10,000 scale), produced by the Portuguese Geographical Institute and by the Geographical Institute of the Military, with the European Terrestrial Reference System coordinated system

(PT-TM06/ETRS89). This is the official data for Portugal and included, among others, the National Geodetic Network and GPS Permanent Network to provide an expected vertical accuracy ranging from 1 to 1.5 m [46]. A triangulated irregular network surface was generated from contour lines through the Delaunay triangulation and was converted to raster with a 10 m × 10 m cell size, in order to respect the contour lines equidistance.

The 1 m resolution DEM was provided by a LiDAR survey (April 2019) with a flight performed at approximately 2792 m with a 30% overlap between sweeps. The point clouds with an average point density of 2 points m^{-2} were captured using Leica ALS80HP, a high performance airborne scanner operating at a pulse rate 704 kHz and scan rate of 73.5 Hz. The airborne laser scanning point clouds were processed and classified using CloudCompare and FUSION/LDV 3.80 software [50,51]. The 1 m gridded surface model was interpolated using the GridSurfaceCreate tool in FUSION/LDV 3.60+. Wooded areas may induce positional errors on DEMs. However, as the planted forest in the catchment follow the same compartments (tree plantation plots) since the late 1950s, it is possible to get several sectors with no vegetation, namely during the periods between clear cuts and new coppice cycle (each 12 years). The operations included regular management of the understory vegetation in-between plantation lines. As a result, the airborne laser scan was able to get the surface information without the canopy interference. Additionally, the canopy density on this planted forest, in association with the unpaved roads and firebreaks networks account for several gaps of vegetation and therefore, exposing the topographic surface, which results in an improved accuracy of the laser scan on the actual surface. The official available input data for the 10 m DEM also benefits from this reducing the eventual elevation errors provided on wooded areas.

The three DEMs represent the topographic surface for an almost 20-year period, as the data began to be collected in the late 1990s (for the 10 m DEM), in the earlier 2000 (for the 30 m DEM) and in 2019 (for the 1 m DEM). As a result, there is a temporal gap in the actual representation of the topographic surface. Nevertheless, no significant geomorphological changes are expected to have occurred in the catchment.

2.3. SWAT Modeling Approach and Calibration Routines

The catchment responses were simulated using the SWAT model, through the ArcGIS interface (ArcSWAT version 2012). In order to assess the influence of the DEMs at different resolutions (1 m, 10 m and 30 m), three independent SWAT models were built up, as each new input DEM requires a single new SWAT model.

In the SWAT model, the stream network definition can be done via DEM by "forcing" the model to define the stream network (DEM-based) or by using a pre-defined shapefile on which each line represents a reach with a unique identification code as well as the flow direction in the sub-basins. Similarly, the watershed delineation may be achieved based on the DEM or by using a pre-defined polygon shapefile. The stream networks were calculated with a D8 hydrological algorithm [52], within the Terrain Analysis Using Digital Elevation Models (TauDEM), which is a set of tools for the analysis of terrain using DEMs. The pre-defined watershed limit was calculated with the D8 algorithm based on the 1 m DEM.

To assess the accuracy of the stream network three metrics were used: drainage density (Dd = average total stream length/catchment area; a higher value represents a more agglutination of the channels, [53]); sinuosity (S = length of meandering/straight-line distance; ranging from one for a straight line to zero for a curvy line, [54]); vertices index (Vi = number of vertices/total stream length, wherein a close to zero value indicates lower geometry complexity, with no curvy sectors).

As the catchment presents little altimetry variation, the use of a pre-defined stream network and watershed shapefiles were considered rather than using the DEM-based option in the SWAT model.

In addition, back in the early 2000s, a water management strategy was implemented in a flat sector at the Caniceira catchment outlet, to prevent the occurrence of soil waterlogging during the raining season and as to be used as water storage pond in the driest period. As a result, a small retention pond was created and two stream lines were merged, which only left one channel free flowing. On this flat area, the unmistakable geomorphological evidence of the two parallel thalwegs was captured by the fine detailed DEM (1 m resolution) and included in the extracted stream network. These channel lines are linked to the topographic surface but present no relation with the actual flow direction and altered the actual location of the catchment outlet. On the TauDEM-based stream network, there is a partial a gap on the linkage to the man-made pond (oval marker on Figure 2) and a missed representation of the actual stream lines nearby the catchment outlet (highlighted by the rectangle marker on Figure 2), which impact the outlet location. As a consequence, the stream lines shapefile (.shp) was edited using the ArcGIS Editing toolbox, and the polyline vertices rectified and some vertex deleted in order eliminate these incongruences and to redefine the correct flow direction. Additionally, a field survey was done with a Real Time Kinematic GNSS high-accuracy antenna, to provide a set of 225 ground survey-points in order to assess the positional accuracy of the 1 m DEM based stream network, in particular z (elevation) values. The survey-points were acquired with a triple-frequency GNSS receiver (Arrow Gold antenna) linked to the Portuguese active GNSS network (RENEP). The reference ellipsoid is the GRS80, the coordinate reference system is the ETRS89/PT-TM06 (EPSG:3763) and the vertical heights are based on the GeodPT08 geoid model.

This validation procedure insures a more realistic representation of the flow direction on this flat terminal sector and the definition of a more precise location of the gauged catchment outlet, ultimately leading to an accurate representation of the catchments responses and an improved robustness of the SWAT model. It is worth stressing that the extracted stream network represents channel lines according to the topographic surface, but does not necessarily mean free flow on all channels, as for present day conditions the catchment is facing water scarcity constrains. Figure 2 presents the TauDEM based stream network (dotted line) and the rectified (edited) stream network for the flat terminal sector of the catchment.

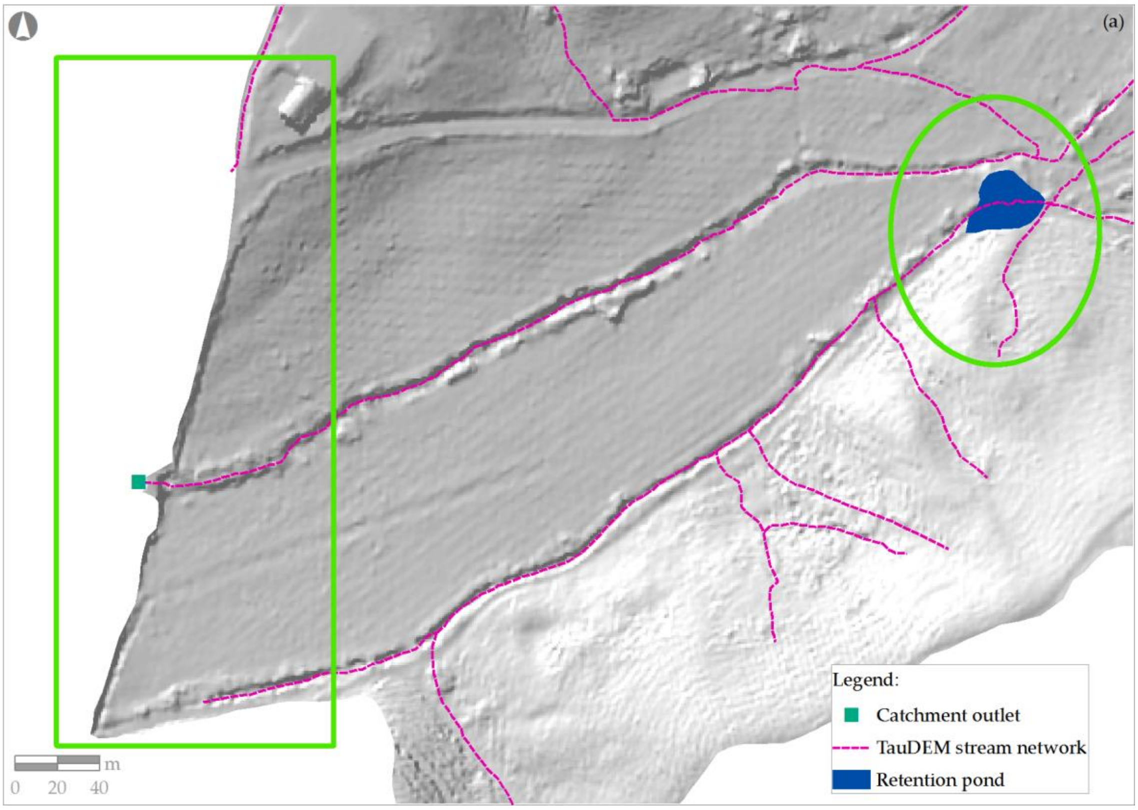

Figure 2. *Cont.*

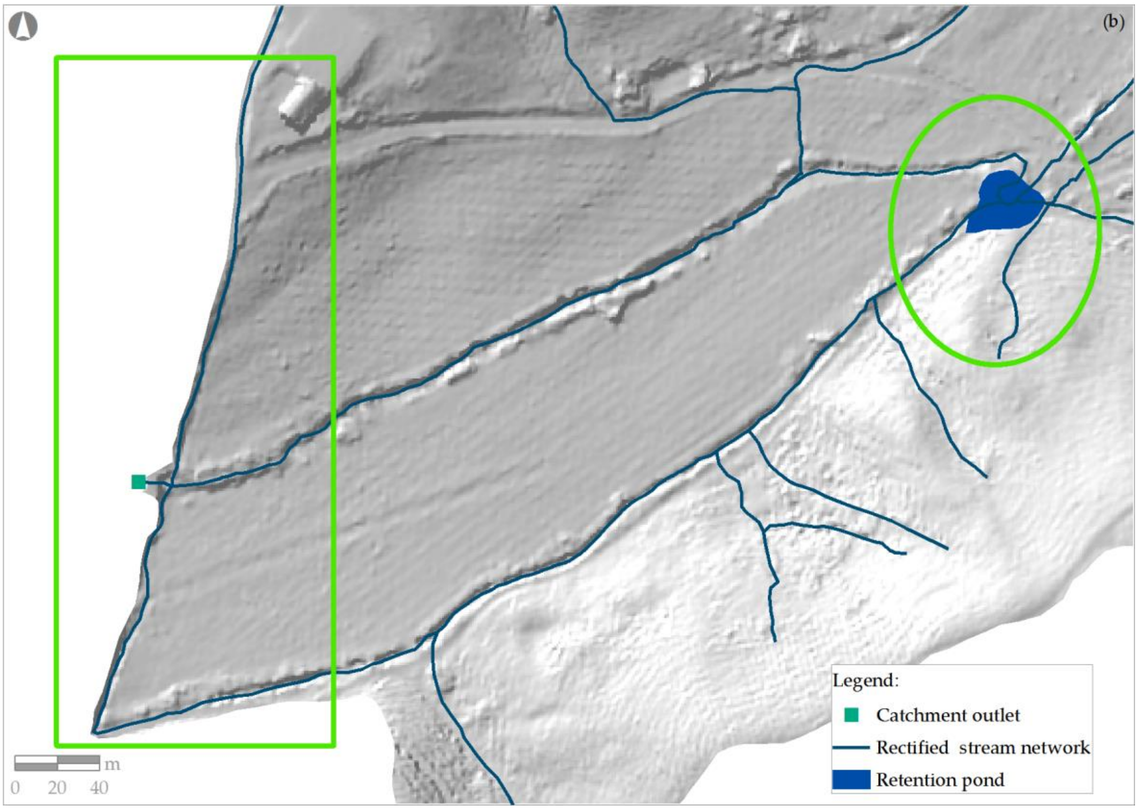

Figure 2. TauDEM generated (**a**) and rectified stream network (**b**), on the flat terminal sector of the catchment for the 1 m DEM resolution, with major differences highlighted in green.

SWAT defines sets of hydrological response units (HRUs) as a unique combination of overlaying land use, soil type and slope for a sub-basin. In the SWAT+ (a revised SWAT version), it is possible to separate water and other land areas per sub-basin (in contrary to the previous SWAT model) and, from the landscape units (LSUs), it is possible to define the HRUs [55].

SWAT is mainly divided in two phases: land phase and routing (water) phase. Within the land phase the amount of water and sediments is controlled, as well as nutrients loads in the main channel for each sub-basin; on the routing phase the movement of water, sediments and nutrients in the stream network throughout the watershed catchment is controlled [56].

To run the model, some input data are mandatory: soil, land cover and crop/plant parameters and climate records.

Soil data resulted of a sampling survey of a minimum of five soil samples per hectare. All samples were analyzed in the laboratory in order to define a comprehensive database of soil physical and chemical characteristics (namely texture, pH, exchangeable cations).

Specific-site parameters for eucalyptus trees were provided by forest inventories, Scholander pressure chamber, leaf area index surveys, sap flow sensors and dendrometers. Eco-physiological data for the other land uses were adapted from the SWAT database and also following previous research [57–60].

The meteorological sub-daily data (precipitation, air temperature, humidity, solar radiation and wind), were provided by two automatic meteorological stations installed in the catchment area since 2012. Sub-daily hydrological records were provided by an automatic stream flow gauge installed in 2019 in a weir open channel at the catchment outlet.

The SWAT management operations database included information on several operations (e.g., soil tillage, planting and maintenance fertilizations, harvesting procedures) that may have influenced the plant growing cycle and the catchment hydrological responses. Plant growth was calculated using a modified version of the Environmental Policy Integrated Calculator (EPIC) crop model [61]. The model simulates the evolution of leaf area index, biomass accumulation as well as the yield for different plants. A detailed operation schedule (for eucalyptus) was defined by date (adapted to local meteorological conditions) rather than by heat units. In addition, refined SWAT parameters (e.g., plantation dates, tillage operations, planting and maintenance fertilizations, weed control, plant growth cycle, leaf area index) were included in the model database based on the long term (50 years) management operations held at Caniceira and also following previous research [57–60]. The model was run on a daily basis from 2012 to 2020 with a warm-up period of five years to minimize the effect of the initial systems variables ensuring proper model dynamic equilibrium.

Calibration routines were performed with Calibration and Uncertainty Analysis Program (SWAT-CUP [62,63]). SWAT-CUP is an iterative calibration procedure that allows the selection of five optimization algorithms and different objective functions (10 in total) and on which multiple variables (parameters) can be assumed and simultaneously calibrated, whether meant for a specific HRU or a set of HRUs or sub-basins. For the Caniceira catchment, a total of 12 sub-basins were considered. The Sequential Uncertainty Fitting algorithm (SUFI2) produces a set of good solutions within the considered parameters and their ranges, and for each iteration, the arrays were gradually narrowed through several iterations. The algorithm accounts for potential sources of uncertainty and helps to determine the most impacting parameters. The calibration was performed for each SWAT model (1 m, 10 m and 30 m resolution DEMs) on two iterations, each with 450 simulations.

Model performance (observed versus calibrated data) was evaluated using three indicators: (i) the Coefficient of Determination (R^2) multiplied by the coefficient of the regression line (bR^2); (ii) the Nash-Sutcliffe model efficiency index (NSE); (iii) the average percent model error (Pbias—percentage of bias) [64–67] (Table 2). The calibration results are expressed from the unsatisfactory to the very good performance rating, following the goodness-of-fit indicators proposed by Moriasi et al. [66].

Table 2. Ratings of the goodness-of-fit indicators for model performance (adapted from Moriasi et al. [66].

Performance Rating	bR^2	NSE	Pbias%
Very good	$0.75 < bR^2 \leq 1.00$	$0.75 < NSE \leq 1.00$	Pbias < ±10
Good	$0.65 < bR^2 \leq 0.75$	$0.65 < NSE \leq 0.75$	±10 ≤ Pbias < ±15
Satisfactory	$0.50 < bR^2 \leq 0.65$	$0.50 < NSE \leq 0.65$	±15 ≤ Pbias < ±25
Unsatisfactory	$bR^2 \leq 0.50$	$NSE \leq 0.50$	Pbias ≥ ±25

3. Results and Discussion

3.1. Impacts of DEM Resolution on Surface Representation and Watershed Properties

The watershed limit was calculated in order to assess the impact of increasing resolution on products extracted from different DEMs. The watershed delineation resulted in a total area value ranging from 267 ha (1 m) to 224 ha (30 m). The watershed area on the 30 m DEM results from a non-realistic generalization of watershed limit due to a super pixel cell size (30 m × 30 m) that accounts for a higher area within the influence of each pixel. Charrier et al. [68] pointed out that the use of very high resolution DEMs could better suit for more realistic watershed delineation, which is true for the 1 m and 10 m resolutions DEMs. In order to avoid these constrains imposed by the DEM resolution on the watershed area, a pre-defined watershed shapefile (calculated with D8 algorithm based on the 1 m DEM) was used in the model. Luo et al. [69] used a pre-defined set of watershed and stream shapefiles for a plain study-area and obtained an improved representation of the actual surface and also increased model accuracy, when compared with a DEM "forcing" procedure.

This resulted in a more realistic representation of the catchment (Figure 3), especially as it is located on a relatively flatten area with low amplitude on elevation values, in line with Luo et al. [69]. A reduction in total watershed area and linked geometry can be substantial, especially on low to medium size watersheds, as the proper representation of the surface and catchment responses is, therefore, affected. A closer analysis points to some incongruence whether due to the lack of detail on catchment headwaters or due to erroneous flow patch and direction calculations on more flat sectors. In addition, loss in detail from altimetry values for coarse resolutions DEMs resulted in an underestimation of the maximum value and an overestimation of the lower catchment altimetry values (Table 3), in line with results reported by Lin et al. [48], Zhang et al. [29] and Reddy et al. [25].

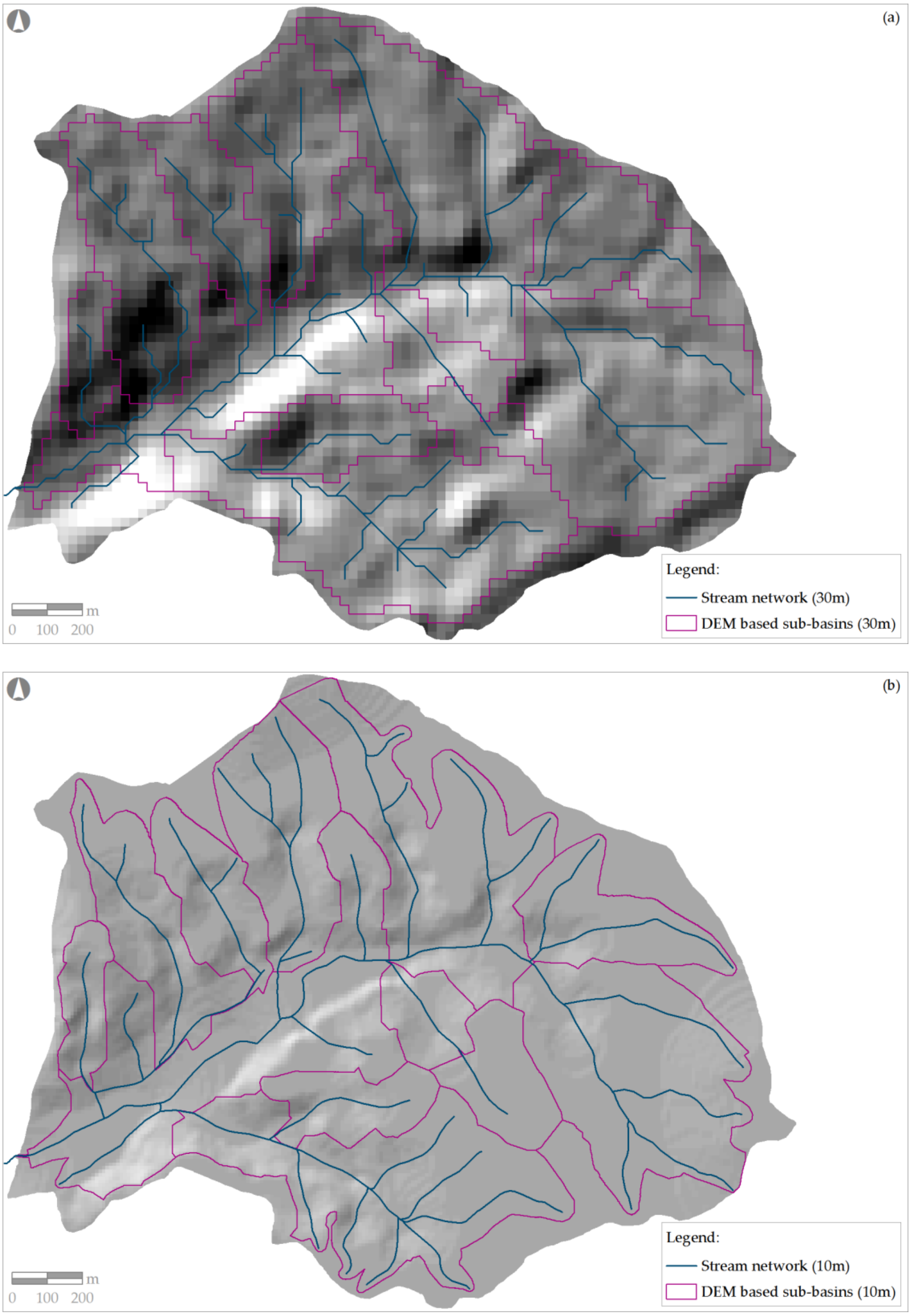

Figure 3. *Cont.*

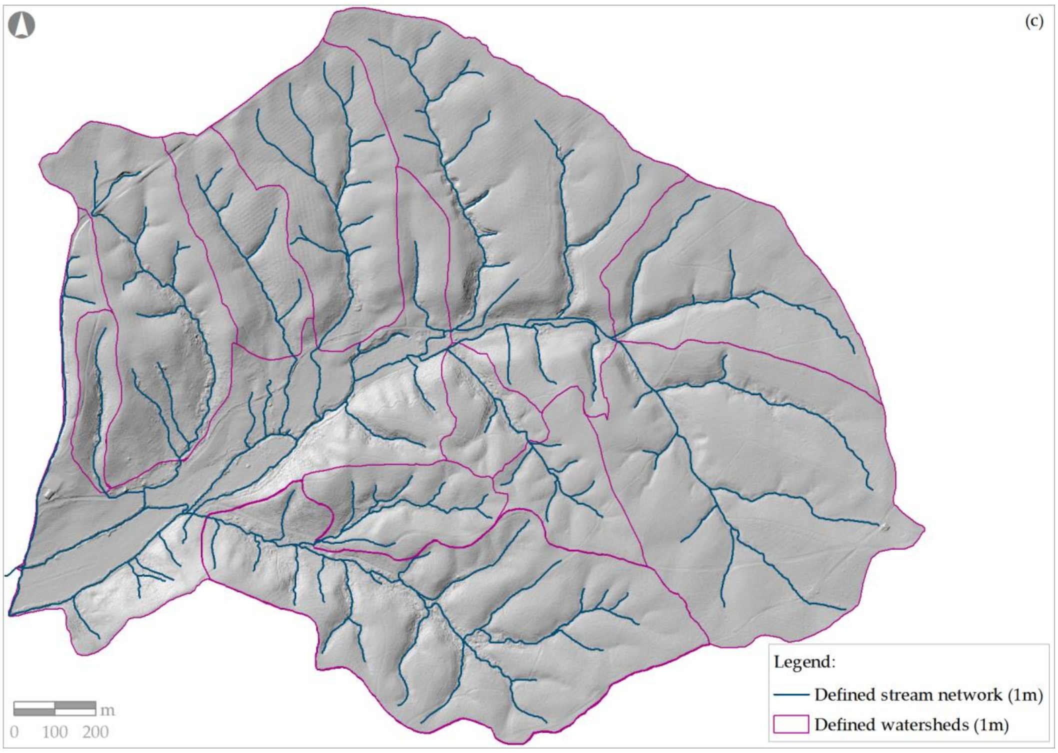

Figure 3. Pre-defined watershed, stream network and DEM-based sub-basins with (**a**) 30 m, (**b**) 10 m and (**c**) 1 m DEM resolution.

Table 3. Caniceira watershed characteristics extracted from 30 m, 10 m and 1 m DEM resolutions.

Watershed Characteristics	**DEM Resolution**		
	30 m	**10 m**	**1 m**
Number of channels	312	735	16,321
Channels length	14,955 m	16,274 m	26,317 m
Strahler order	4	5	7
Elevation (minimum)	105 m	102 m	99 m
Elevation (maximum)	169 m	160 m	164 m
Elevation (Std. deviation)	13.7	11.3	12.8
Drainage density	0.55 mm^{-2}	0.60 mm^{-2}	0.98 mm^{-2}
Sinuosity	0.45	0.12	0.06
Vertices index	0.04	0.09	1.24
Hydrological response units	263	297	402

The accurate three-dimensional representation of a surface is closely related to the resolutions of the input data. In fact, all the 12 sub-basins registered a decrease (from the 1 m to the 30 m resolution) on the number of channels and their length, the Strahler stream order numbers [70] and the slope class values (Table 3).

The 1 m resolution DEM resulted in a significantly higher number of HRUs. The SWAT capability to better simulate surface runoff will be increased as curve numbers will be better adjusted to slope values, based on HRUs slopes, although forest catchments may present a potential higher capability for water storage, as mentioned by Pang et al. [71].

3.2. Impacts of DEM Resolution on Catchment Processes and Responses

The analyses prior to the model calibration intended to obtain insight on the SWAT parameterization to highlight the impact of DEM resolutions, as the three models were built up with the same parameters. The baseline simulation (uncalibrated) on the 1 m DEM embodied a more reduced gap between the observed and simulated data, providing therefore a more realistic representation of the catchment response (bR^2 = 0.74, NSE = 0.58 and Pbias = −40.7). Moreover, observed, simulated (uncalibrated) and calibrated data presented a reduced difference, thus denoting a good overall trend on the model performance (following Moriasi et al. [64]—Table 2), and improved the goodness-of-fit indicators after calibration (bR^2 = 0.87, NSE = 0.84 and Pbias = −14.1). This translates into a better timing of the flow, improved volume simulation and significantly less underestimation of the flow.

The baseline simulations from the 10 m and 30 m resolutions denoted a gradual increase on the gap between observed and simulated. The overall model performance before calibration, based on the bR^2 (0.71 and 0.60, respectively) and NSE index (0.51 and 0.49, respectively) are nevertheless good (Table 4). The Pbias for 10 m and 30 m DEMs indicates an overall flow underestimation (−44.1 and −50.6, respectively) that may be related to the challenges of capturing the total rainfall amounts on extreme precipitation events. As expected, after calibration these values improved.

Table 4. Goodness-of-fit indicators for daily discharge at the Caniceira catchment outlet considering DEM at different resolutions before and after SWAT model calibration. bR^2—ranging from the optimal value (one) to zero; NSE—ranging from the optimal value (one) to zero (below zero indicates unacceptable model simulation); —ranging from the optimal value (zero) to positive or negative values representing model underestimation and overestimation, respectively.

	bR^2			**NSE**			**Pbias**		
DEM Resolution	**30 m**	**10 m**	**1 m**	**30 m**	**10 m**	**1 m**	**30 m**	**10 m**	**1 m**
Uncalibrated	0.60	0.71	0.74	0.49	0.51	0.58	−50.6	−44.1	−40.7
Calibrated	0.85	0.85	0.87	0.60	0.67	0.84	−38.7	−27.0	−14.1

Model simulations showed a gradual deterioration on model performance as DEM moved from 1 m, 10 m to 30 m resolution. This is translated in a gradual loss on accuracy for streamflow at the watershed outlet (gauged) (Figure 4). This analysis was performed in two stages: upon model parameterization (uncalibrated flow) and upon model calibration (calibrated flow). From 1 June to 30 September (2019), the catchment received a total of precipitation as little as 17.8 mm. Upon the first rain events on mid-October, the responses are showed at the catchment outlet where the river gauge and model outlet are located. The extreme precipitation event in December 2019 affecting Portugal ("Elsa storm") resulted in the highest flow peak visible on both stages hydrographs. The hydrological response provided by the flow peak denotes a higher peak representation for the 1 m DEM and a gradual decrease on peak representation for coarser resolutions. The catchment meteorological stations registered 114.4 mm of rain, respectively, with 68.4 mm on the 19th of December and 46.0 mm on the 20th of December (2019).

On this forest dominated Mediterranean catchment with low elevation range, the SWAT modeling of the responses to intense precipitation events have clearly showed a better fit using very high resolution DEM, either uncalibrated or calibrated, and can, therefore, be considered a very good model performance based on bR^2 and NSE, and a satisfactory performance based on Pbias [66,67].

Reddy et al. [25] found similar relation with different resolution DEM and stressed that accuracy of estimated runoff and sediment yield decreases with coarser resolutions. The rational for using coarse DEM resolutions has been largely discussed by several authors [6,72]. They concluded that despite poor accuracy, they present a reasonable compromise between available (freely) data and low computation demands and a suitable representation of hydrological processes and catchment responses, in the context of hydrological model simulations. The findings of the present work contrast some previous studies [28–31,73] that showed that high resolutions DEM have a negligible effect on streamflow reduction. As suggested by Tan el al. [13], such studies rely on coarser DEM resolutions. In addition, most models are calibrated using monthly to yearly records, which may uncover some short-term discharge tendencies, event-based responses and peak flow representations. Finally, fine DEM resolutions may not add any significant advantage in flow representation of large watersheds and in mountain areas [29].

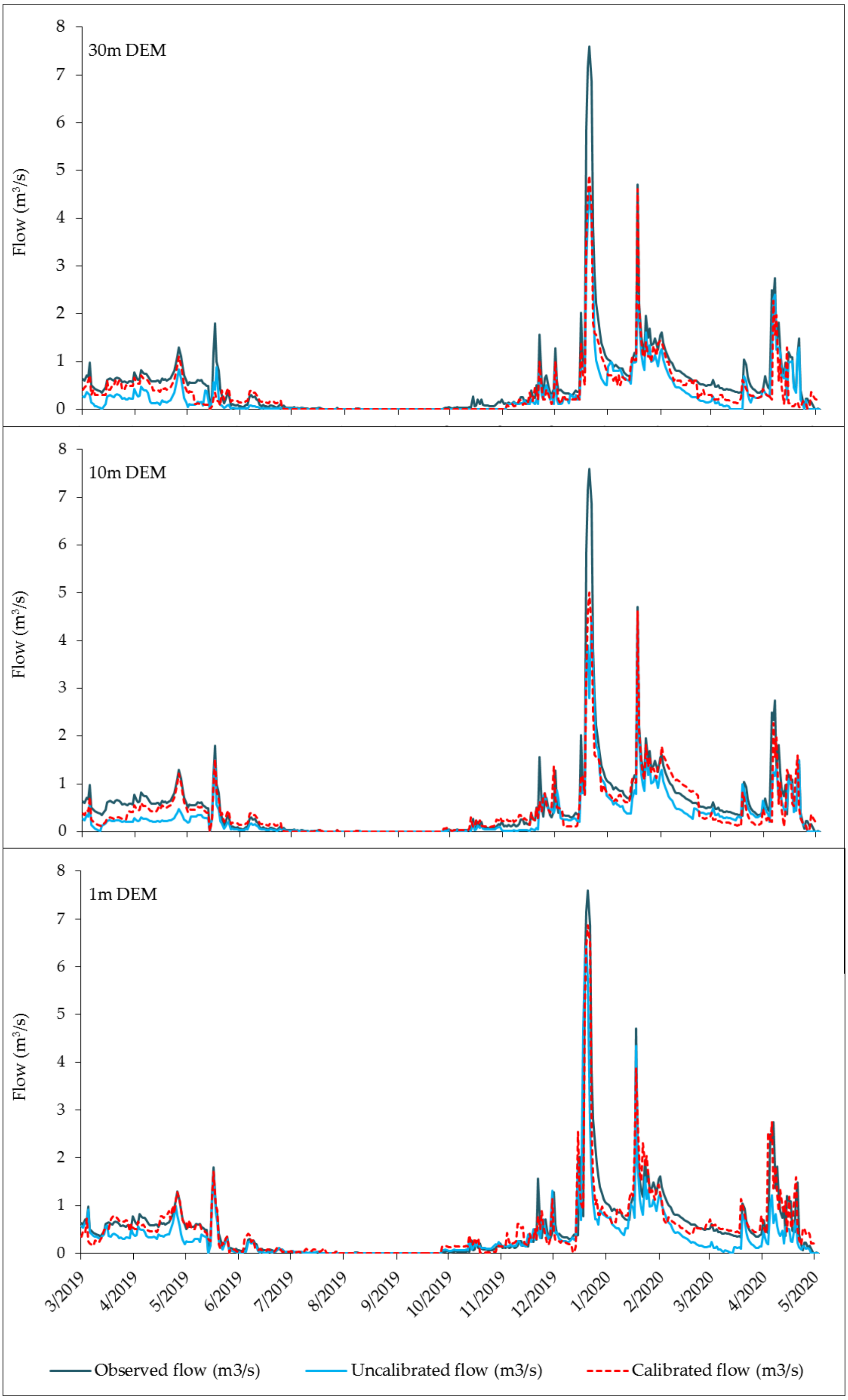

Figure 4. SWAT model performance for uncalibrated and calibrated flows for Caniceira catchment, for the three DEM resolutions.

A more detailed representation of the terrain supports the definition of site-specific forestry operations, better planning of LULC, stands location site-indices and stocking and harvesting operations. High resolution DEM can also be used in support the planning of forest roads and drainage infrastructures, in order to prevent biotic, waterlogging and forest fire risks.

On one hand, future work must be conducted in order to assess the real value for forest planning of modeling with fine resolution DEM, since fine detail DEM are often not freely available. On the other hand, future research may consider the use of SWAT model to simulate adaptive land management strategies to improve the resilience of stands to water scarcity, particularly in the context of climate change scenarios.

4. Conclusions

The study looked into two major research questions: (i) What is the impact of different DEM resolutions on surface representation and watershed properties in a flat area? (ii) Is it worthwhile to use very high resolution DEMs to simulate catchment processes and responses in a forest dominated catchment under the influence of Mediterranean climate?

In the low-relief Caniceira forest catchment with a low altimetry variation, the use of high resolution DEM resulted in an improved representation of the surface with a more accurate report of watershed characteristics, namely, the number and length of channels and the Strahler order. At the flat end sector of the catchment, the high detail DEM (1 m) generated two parallel channels with significance on the morphological representation but with no linkage to the actual water direction. The 1 m DEM was able to capture water bodies (ponds) and the tree plantation lines. Moreover, the coarse resolutions DEMs fail to capture these topographic evidences. The detailed input from 1 m DEM is better suited to model the hydrological response of this catchment, located in a water scarce region of Portugal (under the influence of Mediterranean climate). In fact, the model performance was increasingly improved as fine resolutions DEMs were implemented allowing a better representation of actual processes and events, such as better timing of the flow, improved volume simulation and significantly less underestimation of the flow.

Author Contributions: Conceptualization, J.R. and A.Q.; Data curation, J.R.; Formal analysis, J.R. and A.D.; Investigation, J.R. and A.Q.; Methodology, J.R. and A.Q.; Software, J.R. and A.D.; Validation, J.R.; Visualization, J.R.; Resources, M.S., J.V. and A.Q.; Project administration S.F. and A.Q.; Funding acquisition, M.S.; Supervision, S.F. and A.Q.; Writing—original draft, J.R. and A.Q.; Writing—review and editing, J.R., A.D., S.F., J.A., B.R.-R. and A.Q. All authors have read and agreed to the published version of the manuscript.

Funding: This study has been developed within the context of MySustainableForest project, which has received funding from the European Union's Horizon 2020 research and innovation program under grant agreement No 776045.

Acknowledgments: The authors would like to express appreciation to the efforts from Bruna Scarparo, Célia Fernandes, Fernando Arede and Filipe Louro on data collection and hydrological survey. The authors would like to express appreciation to Nuno Borralho for the revisions and English language correction.

Conflicts of Interest: The authors declare no conflict of interest.

References

1. Stape, J.L.; Binkley, D.; Ryan, M.G.; Fonseca, S.; Loos, R.A.; Takahashi, E.N.; Silva, C.R.; Silva, S.R.; Hakamada, R.E.; Ferreira, J.M.A.; et al. The Brazil Eucalyptus Potential Productivity Project: Influence of water, nutrients and stand uniformity on wood production. *For. Ecol. Manage.* **2010**, *259*, 1684–1694. [CrossRef]
2. Peel, M.C.; Finlayson, B.L.; McMahon, T.A. Updated world map of the Köppen-Geiger climate classification. *Hydrol. Earth Syst. Sci.* **2007**, *11*, 1633–1644. [CrossRef]
3. Spinoni, J.; Vogt, J.; Naumann, G.; Carrao, H.; Barbosa, P. Towards identifying areas at climatological risk of desertification using the Köppen-Geiger classification and FAO aridity index. *Int. J. Climatol.* **2015**, *35*, 2210–2222. [CrossRef]

4. *IFN6–6º Inventário Florestal Nacional*; Instituto da Conservação da Natureza e das Florestas: Lisboa, Portugal, 2019. (In Portuguese)
5. Sofia, G. Combining Geomorphometry, Feature Extraction Techniques and Earth-Surface Processes Research: The Way Forward. *Geomorphology* **2020**, *355*, 107055. [CrossRef]
6. Zhang, W.; Montgomery, D.R. Digital elevation model grid size, landscape representation, and hydrologic simulations. *Water Resour. Res.* **1994**, *30*, 1019–1028. [CrossRef]
7. Burrough, P.A.; Macdonnell, R.A.; Lloyd, C.D. *Principles of Geographical Information Systems*, 3rd ed.; Oxford University Press: New York, NY, USA, 2015; p. 352.
8. Florinsky, I.V. *Digital Terrain Analysis in Soil Science and Geology*, 2nd ed.; Elsevier Academic Press: Amsterdam, The Netherlands, 2016; p. 379.
9. Ouédraogo, M.; Degré, A.; Debouche, C.; Lisein, J. The evaluation of unmanned aerial system-based photogrammetry and terrestrial laser scanning to generate DEMs of agricultural watersheds. *Geomorphology* **2014**, *214*, 339–355. [CrossRef]
10. Muhadi, N.A.; Abdullah, A.F.; Bejo, S.K.; Mahadi, M.R.; Mijic, A. The Use of LiDAR-Derived DEM in Flood Applications: A Review. *Remote Sens.* **2020**, *12*, 2308. [CrossRef]
11. Sørensen, R.; Seibert, J. Effects of DEM resolution on the calculation of topographical indices: TWI and its components. *J. Hydrol.* **2007**, *347*, 79–89. [CrossRef]
12. Vaze, J.; Teng, T.; Spencer, G. Impact of DEM accuracy and resolution on topographic indices. *Environ. Model. Softw.* **2010**, *25*, 1086–1098. [CrossRef]
13. Tan, M.L.; Ficklin, D.L.; Dixon, B.; Ibrahim, A.L.; Yusop, Z.; Chaplot, V. Impacts of DEM resolution, source, and resampling technique on SWAT-simulated streamflow. *Appl. Geogr.* **2015**, *63*, 357–368. [CrossRef]
14. Tan, M.L.; Ramli, H.P.; Tam, T.H. Effect of DEM resolution, source, resampling technique and area threshold on SWAT outputs. *Water Resour. Manag.* **2018**, *32*, 4591–4606. [CrossRef]
15. Xu, F.; Dong, G.; Wang, Q.; Liu, L.; Yu, W.; Men, C.; Liu, R. Impacts of DEM uncertainties on critical source areas identification for non-point source pollution control based on SWAT model. *J. Hydrol.* **2016**, *540*, 355–367. [CrossRef]
16. McDonald, S.; Mohammed, I.N.; Bolten, J.D.; Pulla, S.; Meechaiya, C.; Markert, A.W.; Srinivasang, R.; Nelson, J.; Lakshmi, V. A web-based decision support system tools: The Soil and Water Assessment Tool online visualization and analyses (SWATOnline) and NASA earth observation data downloading and reformatting tool (NASAaccess). *Environ. Model. Softw.* **2019**, *120*, 104499. [CrossRef] [PubMed]
17. Ferraz, S.F.D.B.; Rodrigues, C.B.; Garcia, L.G.; Alvares, C.A.; Lima, W.D.P. Effects of Eucalyptus plantation on streamflow in Brazil: Moving beyond the water use debate. *For. Ecol. Manage.* **2019**, *453*, 1–10. [CrossRef]
18. Di Luzio, M.; Srinivasan, R.; Arnold, J.G.; Neitsch, S.L. *Soil and Water Assessment Tool–ArcView GIS Interface Manual–Version 2000*; Grassland, Soil and Water Research Laboratory, Agricultural Research Service and Blackland Research Center, Texas Agricultural Experiment Station: Temple, TX, USA, 2001.
19. Arnold, J.G.; Moriasi, D.N.; Gassman, P.W.; Abbaspour, K.C.; White, M.J.; Srinivasan, R.; Santhi, C.; Harmel, R.D.; van Griensven, A.; Van Liew, N.W.; et al. SWAT: Model use, calibration, and validation. *Trans. ASABE* **2012**, *55*, 1491–1508. [CrossRef]
20. CARD 2020. *SWAT Literature Database for Peer-Reviewed Journal Articles*; Center for Agricultural and Rural Development, Iowa State University: Ames, IA, USA, 2019; Available online: https://www.card.iastate.edu/swat_articles/ (accessed on 4 May 2020).
21. Cotter, A.S.; Chaubey, I.; Costello, T.A.; Soerens, T.S.; Nelson, M.A. Water quality model output uncertainty as affected by spatial resolution of input data. *J. Am. Water Resour. Assoc.* **2003**, *39*, 977–986. [CrossRef]
22. Dixon, B.; Earls, J. Resample or not?! Effects of resolution of DEMs in watershed modeling. *Hydrol. Process.* **2009**, *23*, 1714–1724. [CrossRef]
23. Duru, U.; Arabi, M.; Wohl, E.E. Modeling stream flow and sediment yield using the SWAT model: A case study of Ankara River basin, Turkey. *Phys. Geogr.* **2017**, *39*, 264–289. [CrossRef]
24. Goulden, T.; Jamieson, R.; Hopkinson, C.; Sterling, S.; Sinclair, A.; Hebb, D. Sensitivity of hydrological outputs from SWAT to DEM spatial resolution. *Photogramm. Eng. Remote Sens.* **2014**, *80*, 639–652. [CrossRef]
25. Reddy, A.S.; Reddy, M.J. Evaluating the influence of spatial resolutions of DEM on watershed runoff and sediment yield using SWAT. *J. Earth Syst. Sci.* **2015**, *124*, 1517–1529. [CrossRef]
26. Nagaveni, C.; Kumar, K.P.; Ravibabu, M.V. Evaluation of TanDEMx and SRTM DEM on watershed simulated runoff estimation. *J. Earth Syst. Sci.* **2018**, *128*, 2. [CrossRef]

27. Munoth, P.; Goyal, R. Effects of DEM source, spatial resolution and drainage area threshold values on hydrological modeling. *Water Resour. Manag.* **2019**, *33*, 3303–3319. [CrossRef]
28. Lin, S.; Jing, C.; Coles, N.A.; Chaplot, V.; Moore, N.J.; Wu, J. Evaluating DEM source and resolution uncertainties in the Soil and Water Assessment Tool. *Stoch. Environ. Res. Risk Assess.* **2012**, *27*, 209–221. [CrossRef]
29. Zhang, P.; Liu, R.; Bao, Y.; Wang, J.; Yu, W.; Shen, Z. Uncertainty of SWAT model at different DEM resolutions in a large mountainous watershed. *Water Res.* **2014**, *53*, 132–144. [CrossRef]
30. Kumar, B.; Lakshmi, V.; Patra, K.C. Evaluating the Uncertainties in the SWAT Model Outputs due to DEM Grid Size and Resampling Techniques in a Large Himalayan River Basin. *J. Hydrol. Eng.* **2017**, *22*, 04017039. [CrossRef]
31. Goulden, T.; Hopkinson, C.; Jamieson, R.; Sterling, S. Sensitivity of DEM, slope, aspect and watershed attributes to LiDAR measurement uncertainty. *Remote Sens. Environ.* **2016**, *179*, 23–35. [CrossRef]
32. Wu, M.; Shi, P.; Chen, A.; Shen, C.; Wang, P. Impacts of DEM resolution and area threshold value uncertainty on the drainage network derived using SWAT. *Water SA* **2017**, *43*, 450. [CrossRef]
33. Camargos, C.; Julich, S.; Houska, T.; Bach, M.; Breuer, L. Effects of Input Data Content on the Uncertainty of Simulating Water Resources. *Water* **2018**, *10*, 621. [CrossRef]
34. Köppen, W. *Grundriss der Klimakunde*; Walter de Gruyter: Berlin, Germany, 1931; p. 388.
35. Thornthwaite, C.W. An approach toward a rational classification of climate. *Geogr. Rev.* **1948**, *38*, 55–94. [CrossRef]
36. Morais, J. Divisão climática de Portugal. In *Memórias e Notícias*; Publicações do Museu Mineralógico e Geológico da Universidade de Coimbra: Coimbra, Portugal, 1959; p. 27. (In Portuguese)
37. Dias, R.; Araújo, A.; Terrinha, P.; Kullberg, J.C. (Eds.) *Geologia de Portugal. Volume II Geologia Meso-Cenozóica de Portugal*; Escolar Editora: Lisboa, Portugal, 2013; p. 798. (In Portuguese)
38. Gonçalves, F.; Zbyzewski, G.; Carvalhosa, A.; Coelho, A.P. *Notícia Explicativa da Carta Geológica de Portugal na Escala 1/50 000, Folha 27-D*; Serviços Geológicos de Portugal: Lisboa, Portugal, 1979; p. 75. (In Portuguese)
39. Almeida, C.; Jesus, M.R.; Mendonça, J.J.L.; Gomes, A.J. *Sistemas Aquíferos de Portugal Continental-Sistema Aquífero das Aluviões do Tejo*; INAG: Lisboa, Portugal, 2000; p. 12.
40. Matias, M.J.; Marques, J.M.; Figueiredo, P.; Basto, M.J.; Abreu, M.M.; Carreira, P.M.; Ribeiro, C.; Flambo, A.; Feliciano, J.; Vicente, E.M. Assessment of pollution risk ascribed to Santa Margarida Military Camp activities (Portugal). *Environ. Geol.* **2008**, *56*, 1227–1235. [CrossRef]
41. SROA. *Carta dos Solos de Portugal. I Vol: Classificação e Caracterização Morfológica dos Solos*; Ministério da Economia, Secretaria de Estado da Agricultura, Serviço de Reconhecimento e Ordenamento Agrário: Lisboa, Portugal, 1970. (In Portuguese)
42. Cardoso, J.V.J.C. A Classificação dos Solos de Portugal-Nova Versão. *Boletim de Solos (SROA)* **1974**, *17*, 14–46. (In Portuguese)
43. FAO–UNESCO. *Soil Map of the World. Vol. I-Legend*; UNESCO: Paris, France, 1974.
44. FAO–UNESCO. *Soil Map of the World. Revised Legend*; World Soil Resources Report No. 60: Rome, Italy, 1988; p. 59.
45. Rabus, B.; Eineder, M.; Roth, A.; Bamler, R. The Shuttle Radar Topography Mission-A new class of digital elevation models acquired by spaceborne radar. *ISPRS J. Photogramm. Remote Sens.* **2003**, *57*, 241–262. [CrossRef]
46. Gonçalves, J.A.; Fernandes, J.C. *Assessment of SRTM-3 DEM in Portugal with Topographic Map Data*; EARSeL 3D Remote Sensing Workshop: Porto, Portugal, 2005.
47. Gonçalves, J.A.; Morgado, A. Use of the SRTM DEM as a geo-referencing tool by elevation matching. *Int. Arch. Photogramm. Remote Sens. Spat. Inf. Sci.* **2008**, *37*, 879–883.
48. Lin, S.; Jing, C.; Chaplot, X.; Yu, X.; Zhang, Z.; Moore, N.; Wu, J. Effect of DEM resolution on SWAT outputs of runoff, sediment and nutrients. *Hydrol. Earth Syst. Sci.* **2010**, *7*, 4411–4435. [CrossRef]
49. Sharma, A.; Tiwari, K.N. A comparative appraisal of hydrological behavior of SRTM DEM at catchment level. *J. Hydrol.* **2014**, *519*, 1394–1404. [CrossRef]
50. Petrasova, A.; Mitasova, H.; Petras, V.; Jeziorska, J. Fusion of high-resolution DEMs for water flow modeling. *Open Geospat. Data Softw. Stand.* **2017**, *2*, 6. [CrossRef]

51. McGaughey, R.J. *FUSION/LDV: Software for LIDAR Data Analysis and Visualization (Version 3.60+)*; Pacific Northwest Research Station, United States Department of Agriculture Forest Service: Seattle, WA, USA, 2009; p. 123.
52. Tarboton, D.G. A new method for the determination of flow directions and contributing areas in grid digital elevation models. *Water Resour. Res.* **1997**, *33*, 309–319. [CrossRef]
53. Horton, R.E. Erosional development of streams and their drainage basins; hydrophysical approach to quantitative morphology. *Geol. Soc. Am. Bull.* **1945**, *56*, 275–370. [CrossRef]
54. Mueller, J.E. An introduction to the hydraulic and topographic sinuosity indexes. *Ann. Assoc. Am. Geogr.* **1968**, *58*, 371–385. [CrossRef]
55. Bieger, K.; Arnold, J.G.; Rathjens, H.; White, M.J.; Bosch, D.D.; Allen, P.M. Introduction to SWAT+, a Completely Restructured Version of the Soil and Water Assessment Tool. *J. Am. Water Resour. Assoc.* **2016**, *53*, 115–130. [CrossRef]
56. Neitsch, S.L.; Arnold, J.G.; Kiniry, J.R.; Williams, J.R.; King, K.W. *Soil and Water Assessment Tool Theoretical Documentation, Version 2000*; Blackland Research Center, Texas Agricultural Experiment Station: Temple, TX, USA, 2001.
57. Rocha, J.; Roebeling, P.; Rialrivas, M.E. Assessing the impacts of sustainable agricultural practices for water quality improvements in the Vouga catchment (Portugal) using the swat model. *Sci. Total Environ.* **2015**, *536*, 48–58. [CrossRef] [PubMed]
58. Rocha, J.; Carvalho-Santos, C.; Diogo, P.; Beça, P.; Keizer, J.J.; Nunes, J.P. Impacts of climate change on reservoir water availability, quality and irrigation needs in a water scarce Mediterranean region (southern Portugal). *Sci. Total Environ.* **2020**, *736*, 139477. [CrossRef]
59. Serpa, D.; Nunes, J.P.; Santos, J.; Sampaio, E.; Jacinto, R.; Veiga, S.; Lima, J.C.; Moreira, M.; Corte-Real, J.; Keizer, J.J.; et al. Impacts of climate and land use changes on the hydrological and erosion processes of two contrasting Mediterranean catchments. *Sci. Total Environ.* **2015**, *538*, 64–77. [CrossRef]
60. Nunes, J.P.; Jacinto, R.; Keizer, J.J. Combined impacts of climate and socio-economic scenarios on irrigation water availability for a dry Mediterranean reservoir. *Sci. Total Environ.* **2017**, *584–585*, 219–233.
61. Williams, J.R.; Jones, C.A.; Dyke, P.T. A modeling approach to determining the relationship between erosion and soil productivity. *Trans. ASAE* **1984**, *27*, 129–144. [CrossRef]
62. Abbaspour, K.C. *User Manual for SWAT-CUP, SWAT Calibration and Uncertainty Analysis Programs*; Swiss Federal Institute of Aquatic Science and Technology, Eawag: Duebendorf, Switzerland, 2007.
63. Abbaspour, K.C.; Rouholahnejad, E.; Vaghefi, S.; Srinivasan, R.; Yang, H.; Kløve, B. A continental-scale hydrology and water quality model for Europe: Calibration and uncertainty of a high-resolution large-scale SWAT model. *J. Hydrol.* **2015**, *524*, 733–752. [CrossRef]
64. Gupta, H.V.; Sorooshian, S.; Yapo, P.O. Status of automatic calibration for hydrologic models: Comparison with multilevel expert calibration. *J. Hydrol. Eng.* **1999**, *4*, 135–143. [CrossRef]
65. Krause, P.; Boyle, D.; Bäse, P. Comparison of different efficiency criteria for hydrological model assessment. *Adv. Geosci.* **2005**, *5*, 89–97. [CrossRef]
66. Moriasi, D.N.; Arnold, J.G.; Van Liew, M.W.; Bingner, R.L.; Harmel, R.D.; Veith, T.L. Model evaluation guidelines for systematic quantification of accuracy in watershed simulations. *Trans. ASABE* **2007**, *50*, 885–900. [CrossRef]
67. Moriasi, D.N.; Gitau, M.W.; Pai, N.; Daggupati, P. Hydrologic and water quality models: Performance measures and evaluation criteria. *Trans. ASABE* **2015**, *58*, 1763–1785.
68. Charrier, R.; Li, Y. Assessing resolution and source effects of digital elevation models on automated floodplain delineation: A case study from the Camp Creek Watershed, Missouri. *Appl. Geogr.* **2012**, *34*, 38–46. [CrossRef]
69. Luo, Y.; Su, B.; Yuan, J.; Li, H.; Zhang, Q. GIS Techniques for Watershed Delineation of SWAT Model in Plain Polders. *Procedia Environ. Sci.* **2011**, *10*, 2050–2057. [CrossRef]
70. Strahler, A.N. Quantitative analysis of watershed geomorphology. *Trans. Am. Geophys. Union* **1957**, *38*, 913–920. [CrossRef]
71. Pang, S.J.; Wang, X.Y.; Melching, C.S.; Feger, K.H. Development and testing of a modified SWAT model based on slope condition and precipitation intensity. *J. Hydrol.* **2020**, *588*, 125098. [CrossRef]

72. Yang, P.; Ames, D.P.; Fonseca, A.; Anderson, D.; Shrestha, R.; Glenn, N.F.; Cao, Y. What is the effect of LiDAR-derived DEM resolution on large-scale watershed model results? *Environ. Model. Softw.* **2014**, *58*, 48–57. [CrossRef]
73. Malagó, A.; Vigiak, O.; Bouraoui, F.; Pagliero, L.; Franchini, M. The hillslope length impact on SWAT streamflow prediction in large basins. *J. Environ. Inform.* **2018**, *32*, 82–97. [CrossRef]